Electrochimica Acta 184 (2015) 323–330

Contents lists available at ScienceDirect

Electrochimica Acta

journal homepage: www.elsevier.com/locate/electacta

Nitrate and Nitrite Electrocatalytic Reduction at Layer-by-Layer Films Composed of Dawson-type Heteropolyanions Mono-substituted with Transitional Metal Ions and Silver Nanoparticles

Shahzad Imar[a], Mustansara Yaqub[a], Chiara Maccato[b], Calum Dickinson[c], Fathima Laffir[c], Mikhail Vagin[d,e,*], Timothy McCormac[a]

[a] Electrochemistry Research Group, Department of Applied Science, Dundalk Institute of Technology, Dublin Road Dundalk, County Louth, Ireland
[b] Department of Chemistry, University of Padova Via F. Marzolo, 1, 35131 Padova, Italy
[c] Materials and Surface Science Institute, University of Limerick, Limerick, Ireland
[d] Department of Physics, Chemistry and Biology, Linköping University, SE-581 83, Linköping, Sweden
[e] Laboratory of Organic Electronics, Department of Science and Technology, Linköping University, SE-601 74, Norrköping, Sweden

ARTICLE INFO

Article history:
Received 14 September 2015
Received in revised form 8 October 2015
Accepted 16 October 2015
Available online 20 October 2015

Keywords:
Mono-substituted heteropolyanions
nitrate reduction
silver nanoparticles
electrocatalysis
layer-by-layer assembly

ABSTRACT

A series of Dawson-type heteropolyanions (HPAs) mono-substituted with transitional metal ions ($_{\alpha 2}$-$[P_2W_{17}O_{61}Fe^{III}]^{8-}$, $_{\alpha 2}$-$[P_2W_{17}O_{61}Cu^{II}]^{8-}$ and $_{\alpha 2}$-$[P_2W_{17}O_{61}Ni^{II}]^{8-}$) have exhibited electrocatalytic properties towards nitrate and nitrite reduction in slightly acidic media (pH 4.5). The immobilization of these HPAs into water-processable films developed via layer-by layer assembly with polymer-stabilized silver nanoparticles led to the fabrication of the electrocatalytic interfaces for both nitrate and nitrite reduction. The LBL assembly as well as the changes in the HPA properties by immobilization has been characterized by electrochemical methods. The effects of the substituent ions, outer layers and the cationic moieties utilized for the films assembly of the developed film on the performances of nitrate electrocatalysis has been elucidated.

1. Introduction

Inorganic and organic compounds of nitrogen are one of the most abundant in the human body and are involved in many biological, environmental and industrial processes. In nature, the nitrogen cycle controls the reaction pathways of inorganic compounds of nitrogen. The human alteration substantially alters the nitrogen cycle caused the general increase of both availability and the mobility of nitrogen over large terrestrial regions [1]. Inappropriate drainage of waste water and over-manuring with natural and synthetic fertilizers is becoming a severe environmental concern [2–5]. In particular, being the main source of the drinking water, ground waters are characterized worldwide as having increased nitrate concentration [6]. Being extensively used in industrial [7] and biomedical applications [8–10], nitrite is one of the most reactive substances in the nitrogen cycle and has a significant toxicity for humans, being the main cause of blue baby syndrome [11]. Consumed nitrate is also reduced to nitrite by enteric bacteria, which might subsequently lead to serious health risks [12,13]. The maximum admissible concentrations for nitrates in drinking water is 50 mg/l (0.8 mM) in the European Drinking Water Directive [14–16].

The technologies for nitrate elimination from water are classified into physico-chemical, biological and catalytical processes [15,17]. Being preferred for economical reasons, physico-chemical techniques such as ion exchange, reverse osmosis and electrodialysis do not convert nitrate to harmless compounds but only remove it from the water. Heterogeneously catalyzed nitrate reduction reaction (NRR) to nitrogen for groundwater remediation has been developed [18–20] as one of the alternatives. Biological denitrification is costly, complex and a slow process accompanied with a co-production of large quantities of sludge [4382]. Electrochemical techniques of denitrification via NRR have attracted special interest because of the possibility of operation in high nitrate concentrations [4,20]. The electrode materials that reveal high activity in NRR are limited to noble metals and their bimetallic alloys [4,20] as well as graphene [21]. However, most of these electrocatalytical systems require high acidity [4] or alkalinity [22,23] for effective NRR. The electrocatalysis of NRR has been observed on electrodes functionalized with transition

* Corresponding author. Tel.: +46702753087.
E-mail address: mikva@ifm.liu.se (M. Vagin).

http://dx.doi.org/10.1016/j.electacta.2015.10.082
0013-4686/

metal ions cyclams at rather negative potentials (ca. -1.4 V vs SCE) [24–29].

Heteropolyanions (HPA) are a well-known class of inorganic metal oxygen cluster compounds, which possess excellent electrochemical properties, enabling them to accept and donate multiple electrons reversibly without decomposition. This redox feature renders the HPA excellent electrocatalysts for a variety of substrates [30–32]. Different strategies for the immobilization of HPAs into thin films on electrode surfaces have been adopted [30,33–35], with particular attention being afforded to the employment of the Layer-by-Layer (LBL) technique. This technique is based upon the electrostatic interaction between oppositely charged species from dilute solution [36–38]. Nanocomposite materials which are based on inorganic nanoparticles and polymers offer unique properties, such as, optical, magnetic, catalytic, thermal and electrochemical, which depend on particle size, shape, dimensions and surrounding environment [39–43]. The unusual properties of metallic nanoparticles are due to the collection of high energy surface atoms compared to the bulk solid material.

HPAs have been previously shown to be effective electrocatalysts for the reduction of nitrite [34,44–47] as a standard reaction for the assessment of HPA electrocatalytic performance [48]. Rare examples of transitional metal ion-substituted HPAs demonstrated the electrocatalytic activity towards NRR in mild acidic media (approx. pH 5) [49–56]. The accumulation of transitional ion centers within the HPA cage is associated with an enhancement of the catalytic properties of these atoms, with the complementary advantage to generate highly reduced products by the electrons from the reduced W-O framework as electronic storage [31]. The favorable effect on NRR catalysis of accumulation of substituent ion within the same molecule has been shown for sandwich-type Cu^{2+}- [52] and Ni^{2+}-multisubstituted HPA [52,57] in comparison with monosubstituted derivatives. Starting with the reduction to nitrite by the HPA, the whole reaction goes through nitric oxide (NO) [55] down to ammonia [48]. The significant cathodic overpotential up to 750 mV is observed for NRR electrocatalysis with HPA in comparison with nitrite reduction illustrating the low reactivity of the nitrate ion [49]. Recently we reported the achievement of NRR at the same potential as nitrite reduction observed on crown-type HPA multisubstituted with Cu^{2+} or Ni^{2+} ions immobilized via LBL assembly with silver nanoparticles (AgNP) [58].

In this paper, we report the studies of NRR happened at the same potential as nitrite reduction wave achieved on Dawson-type HPA mono-substituted with transitional metal ions and immobilized via LBL assembly with polymer-stabilized AgNPs. The influence of the incorporated AgNPs on the film's properties and performance has been studied by electrochemical and physical methods. It has been found that the outer layer of the LBL assembly strongly affects the morphological and electrocatalytic properties of films with suficient enhancement of film's electrocatalytic ability being observed with AgNP incorporation.

2. Experimental

2.1. Materials

The lacunary α/β-$K_{10}[P_2W_{17}O_{61}]^{10-}$ Dawson-type HPA was synthesised and characterised according to the literature [59]. The potassium salts of the transition metal ion-substituted $_{\alpha 2}$-$[P_2W_{17}O_{61}Fe^{III}]^{8-}$, $_{\alpha 2}$-$[P_2W_{17}O_{61}Cu^{II}]^{8-}$ and $_{\alpha 2}$-$[P_2W_{17}O_{61}Ni^{II}]^{8-}$ Dawson HPA were synthesised according to the literature [60]. Potassium ferricyanide, potassium ferrocyanide, hexaammineruthenim(III) chloride, silver nitrate (99.99%), poly(ethyleneimine) (PEI, MW ~ 25,000), poly(sodium 4-styrenesulphonate) (PSS, MW ~ 70, 000), poly(diallyldimethylammonium chloride) (PDDA, MW ~ 20, 000) and all the other chemicals were purchased from Sigma–Aldrich. Highly purified water with a resistivity 18.2 MΩ cm (ELGA PURELAB Option-Q) was used for the preparation of all the electrolytes and buffer solutions. The following solutions have been used for the measurements: 0.1 M Na_2SO_4 (the pH was adjusted to 2–3), 0.1 M Na_2SO_4 + 20 mM CH_3COOH (the pH was adjusted to pH 3.5–5), 0.1 M Na_2SO_4 + 20 mM NaH_2PO_4 (the pH was adjusted to pH 5.5–7). The pH of the solutions was adjusted with either 0.1 M NaOH or 0.1 M H_2SO_4.

2.2. Instrumentation

UV-Vis spectra were recorded on a UV-1800 Shimadzu Spectrophotometer in conjunction with quartz cells with path lengths of 1 cm. Scanning electron microscopy (SEM) images were obtained with a Hitachi SU-70. X-ray photoelectron spectroscopy (XPS) was done with a Karatos AXIS-165, Monochromatic Al Kα radiation of energy 1486.58 eV. High resolution spectra were taken at a fixed pass energy of 20 eV. Morphological analysis was carried out on a Zeiss SUPRA 40VP, Field Emission-Scanning Electron Microscopy (FE-SEM), by setting the acceleration voltages at 10 kV.

2.3. Preparation of PEI-stabilized AgNP

A mixture of 100 ml of a 10 mM solution of $AgNO_3$ and 3 ml of 2% (W/W) PEI was heated for 15 minutes with constant stirring. A brown colloidal solution was obtained without precipitation [61].

2.4. Electrochemical procedure

All electrochemical experiments were performed with a CHI660 electrochemical work station employing a conventional three-electrode electrochemical cell. A glassy carbon electrode (GCE, 3 mm diameter, surface area 0.0707 cm^2) was used as the working electrode, a platinum wire as the auxiliary electrode, and a silver/silver chloride as the reference electrode (3 M KCl) in aqueous media in all experiments unless otherwise stated. Prior to use the working electrode was successively polished with 1.0, 0.3 and 0.05 μm alumina powders and sonicated in water for 10 min after each polishing step. Finally, the electrode was washed with ethanol and then dried with a high purity argon stream. All solutions were degassed for 20 min with high purity argon and kept under a blanket of argon during all electrochemical experiments.

2.5. Layer-by-layer (LBL) assembly

A freshly polished GCE was immersed in the 8% (v/v) PDDA solution for 30 minutes for initial surface modification. The electrode was then rinsed thoroughly with deionised water and dipped in a 3.4 mM solution of the corresponding HPA in pH 2 buffer solution for 20 minutes to allow the initial anionic layer to adsorb (Step 1). The modified electrode was rinsed again thoroughly with deionised water and dried with a high purity nitrogen stream. This yielded the PDDA/HPA modified electrodes, which were then dipped in a water solution of AgNP for 20 minutes (Step 2). The electrode was then washed and dried with nitrogen. To build the desired number of layers, steps 1 and 2 were repeated in a cyclic fashion. The outer layer of the multilayer assembly was chosen so as to be either anionic or cationic in nature.

2.6. Electrochemical Impedance Spectroscopy (EIS)

Electrochemical impedance spectroscopy was undertaken employing a 10 mM potassium ferricyanide and 10 mM potassium

ferrocyanide solution in 0.1 M KCl at an applied potential of +230 mV (versus Ag/AgCl) from 0.1 to 10^5 Hz with a voltage amplitude of 10 mV.

3. Results and Discussion

3.1. Characterization of AgNP by UV–vis spectroscopy

PEI was used for the synthesis and stabilization of the AgNP as it has the ability to chelate a variety of transition metal ions with amine groups [62], especially silver ions [63]. The resulting brown colour of the solution obtained during the AgNP synthesis is evidence of the formation of the AgNP. The UV–vis spectroscopy showed the strong absorption band at 408 nm which corresponds to surface plasmon resonance peak of spherical AgNP [31,64].

3.2. Redox Properties of HPA

3.2.1. Solution Phase

Fig. 1 shows the resulting cyclic voltammograms obtained for the various Dawson type HPAs in solution. The redox behaviour of the lacunary HPA (Fig. 1A) is characterized by the presence of three reversible pH dependent bi-electronic redox processes (I, II and III) [46] representing the redox activity of the W-O framework, according to equations (I) through to (III).

$$[P_2W_{17}O_{61}]^{10-} + 2e + 2H^+ \Leftrightarrow [H_2P_2W_{17}O_{61}]^{10-} \quad \text{(I)}$$

$$[H_2P_2W_{17}O_{61}]^{10-} + 2e + 2H^+ \Leftrightarrow [H_4P_2W_{17}O_{61}]^{10-} \quad \text{(II)}$$

$$[H_4P_2W_{17}O_{61}]^{10-} + 2e + 2H^+ \Leftrightarrow [H_6P_2W_{17}O_{61}]^{10-} \quad \text{(III)}$$

The redox response of the Cu^{2+}-substituted HPA (Fig. 1B) exhibits an additional sharp oxidation peak centred around 0 V which is associated with the re-oxidation of the reduced Cu^0 centre. In addition, the first reduction peak current of the W-O I redox process is higher than that observed for other HPAs, which reflects the contribution from reduction of Cu^{2+}-center. The presence of the Fe^{3+}-center (Fig. 1C) led to a reversible mono-electronic redox process at 0 V. The voltammetric response of the Ni^{2+}-substituted HPA reveals the splitting of the W-O I redox process only. All of the transition metal substituted HPAs exhibit similar redox activity as that of the lacunary for the W-O redox processes and these are in agreement with the literature [65].

3.2.2. HPA Based LBL films

Fig. 2 shows the resulting cyclic voltammograms obtained for the assembly of LBL layers based upon the various HPAs and the PEI-stabilized AgNPs. What is evident in all of the voltammograms is the continuous increase in the peak currents for the W-O I, II and III redox processes of the HPA with number of layers, which is indicative of the formation of the HPA functionalised LBL films on the electrode surface. The peak-to-peak separations of all the observed W-O redox processes were seen to become smaller upon immobilization in comparison with the HPA's solution behaviour as would be expected for thin layer behaviour, with the latter being observed up to 500 mV/s for the resulting films (data not shown). The mono-electronic redox process Ag^0/Ag^{+1} ($E_{1/2}$ = 0.12 V and ΔEP = 21 mV), for the incorporated AgNPs, showed minor increase in its peak currents during layer construction. A slight anodic shift has been observed for all the W-O-associated redox processes with LBL assembly immobilization relative to the HPA solution response, which illustrates the interactions between the HPA and AgNP within the constructed layers. The peak currents of W-O redox processes observed during LBL assembly are smaller than the values obtained for LBL films based on the multi-substituted

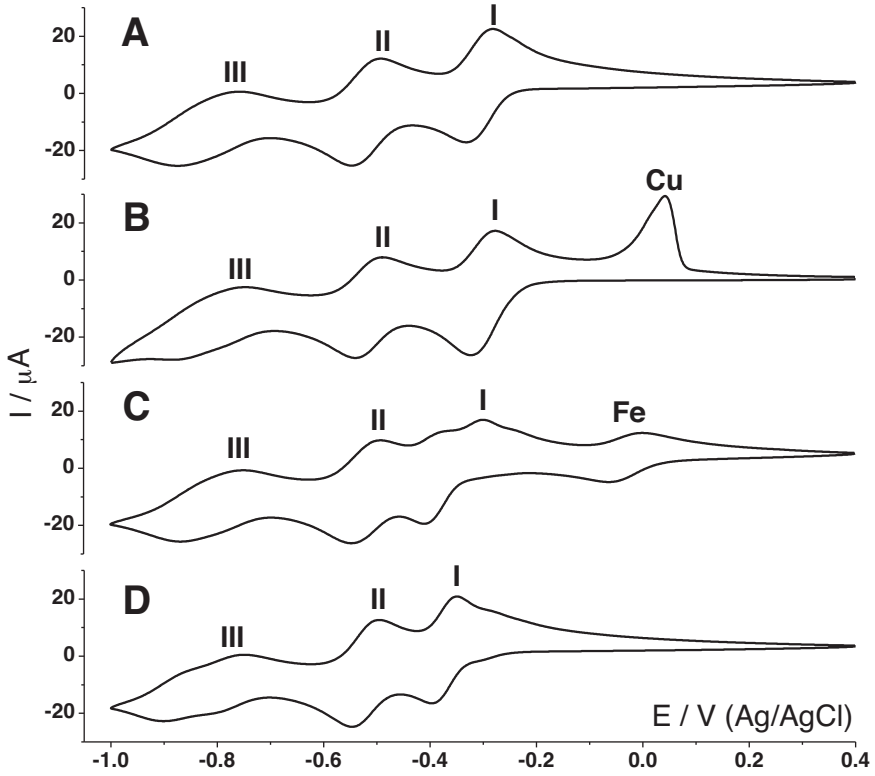

Fig. 1. Voltammetric responses in solution of a series of HPA substituted by different transition metal ions. Cyclic voltammograms were recorded in 1 mM solutions of lacunary and Cu^{2+}-, Fe^{3+} and Ni^{2+}-substituted HPA correspondingly (**A**,**B**,**C** and **D**); pH 3.5, scan rate 100 mV/s.

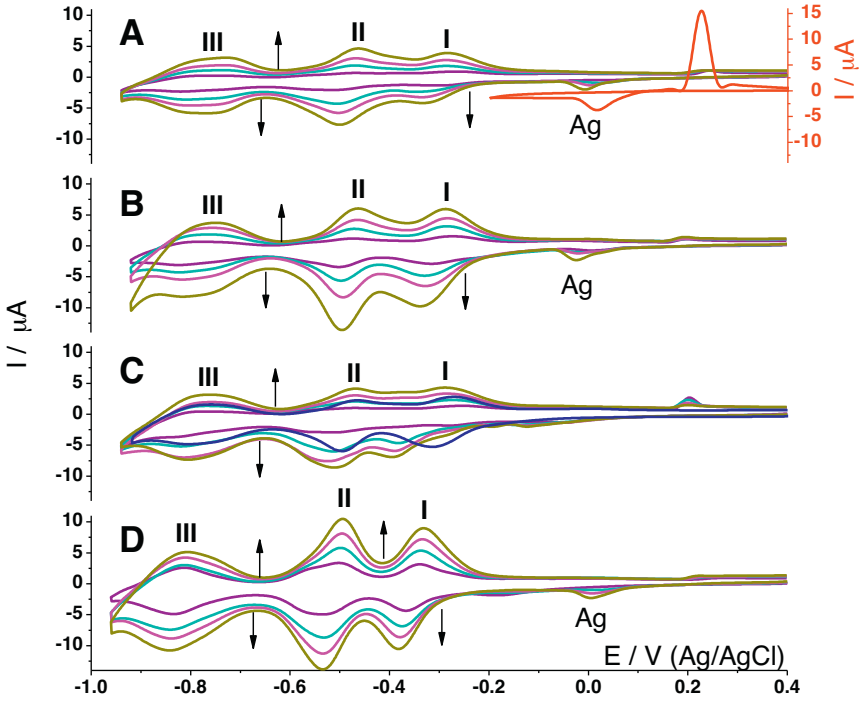

Fig. 2. Assembly HPA-AgNP LBL films monitored by voltammetry. Voltammetric responses were recorded at electrodes modified with films based on lacunary and Cu^{2+}-, Fe^{3+} and Ni^{2+}-substituted HPA (**A,B**, **C** and **D** correspondingly) of different numbers of layers (from 1 to 4) with PEI-stabilized AgNP as a cationic moiety; pH 3.5, scan rate 100 mV/s.. Red curve – voltammetic response of electrode modified with PSS with subsequent modification with PEI-stabilized AgNP; blue curve – voltammogram obtained at electrode modified with LBL film formed from Fe^{3+}-substituted HPA and pristine PEI.

crown-type HPA $[Cu_{20}Cl(OH)_{24}(H_2O)_{12}(P_8W_{48}O_{184})]^{25-}$ and $[Ni_4(P_8W_{48}O_{148})(WO_2)]^{28-}$ [58], which illustrates the effect of the charge of HPA on the assembly efficiency.

Interestingly the redox processes associated with the Cu^{2+}- and Fe^{3+}metal centres in the HPA moieties disappear upon layer formation, which is in agreement with literature data for mono-substituted HPAs [58,66,67] and represents the phenomenon of electrostatic interaction between the HPA and the encapsulating multilayer film. However, the presence of the transition metal ions in the LBL film has been proven through elemental analysis by XPS (Supporting Note 1 and Fig. S1). This effect might be explained by the partial decomposition of the HPA during multilayer construction. Alternatively, the interaction of the HPA with the cationic AgNP can lead to new complex formation characterized with different redox properties [68].

The surface coverage of the resulting LBL films was calculated from the integral charge of the HPA's W-O I anodic peak employing the equation: $\Gamma = Q/nFA$, where Q is the peak charge (C) associated with a particular redox process of the film, n the number of transferred electrons for this redox process, which is equal to 2 for the W-O redox processes of the Dawson-type HPA [46], F is Faraday's constant (96,485C mol^{-1}) and A is the electrode surface area (0.0707 cm^2). The average values of surface coverages were found to be 0.27 nmol cm^{-2}, 0.32 nmol cm^{-2} and 0.39 nmol cm^{-2} for LBL films based on the Cu^{2+}-, Fe^{3+}- and Ni^{2+}-substituted-HPA, respectively.

It has been reported previously that the incorporation of AgNPs into LBL assemblies has led to higher film conductivities [69] or higher efficiencies of assembly, which was revealed from the comparison with the response of LBL film assembled with pure PEI as a cationic moiety (blue curve at Fig. 2C). The voltammetric responses of the LBL film-modified electrodes revealed pH dependence (Fig. S2), which is well-known for HPA [46]. Cathodic shifts of redox potentials observed for the W-O I and II redox processes of the HPA-based LBL films with increasing pH showed the involvement of 2 (in all W-O II and W-O I of Ni^{2+}-subsituted HPA) or 3 protons (in W-O I redox process for Cu^{2+}- and Fe^{3+}-substituted HPA) in the redox step.

3.2.3. Electrochemical impedance spectroscopy (EIS)

The ferro/ferricyanide couple has been used as a redox probe to monitor the LBL assembly process through the employment of EIS. The charge transfer resistance R_{CT}, which represents the electron transfer kinetics of the redox probe, is affected as the underlying electrode surface is modified with varying number of layers during

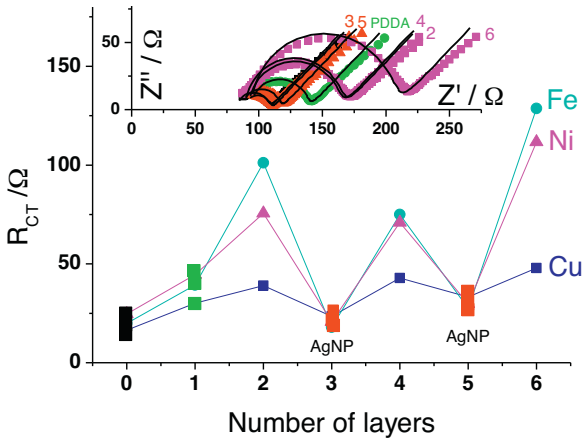

Fig. 3. Assembly HPA-AgNP LBL films monitored by impedance spectroscopy. The dependence of fitted values of charge transfer resistance (RSD 20%) on the number of layers for LBL films assembled from substituted HPA and AgNP. Inset: Nyquist plot of impedance spectra recorded at electrode modified with LBL film of different assembly stages (■ - spectrum of blank electrode; ● - spectrum of PDDA-modified electrode; ▲ - 3 and 5 - spectra of modified electrode after AgNP steps; ■ - 2, 4 and 6 - spectra of modified electrode after Ni^{2+}-substituted HPA steps; solid curves – fitted spectra); 10 mM $K_3[Fe(CN)_6]$, 10 mM $K_4[Fe(CN)_6]$, 0.1 M KCl; 10 mV amplitude, 230 mV potential of measurement.

the LBL construction. R_{CT} can be roughly estimated from the Nyquist plot as the semicircle diameter of the kinetically controlled region at high frequencies (Inset in Fig. 3 and Fig. S3). The equivalent circuit, which consists of a double layer capacitance in series with a solution resistance and in parallel with a branch of diffusion, i.e. charge transfer resistance and Warburg impedance [66], has been applied for the interpretation of the experimental data. Fitting of the experimental data confirmed reproducible switching behaviour of the charge transfer resistance with the outer layers (Fig. 3) for all HPAs. The deposition of AgNP or HPA layers leads to a consistent decrease or increase in R_{CT} respectively, which is consistent with our previous studies [58] and is also confirmed by cyclic voltammetric measurements (data not shown). Firstly, this effect can be probably due to the high conductivity of the metal nanoparticles, which facilitate the electronic communication between the probe molecules and the underlying electrode surface [69,70]. Secondly, the electrostatic attraction between the cationic outer nanoparticles and the negatively charged ferricyanide/ferrocyanide redox probe can increase the electrode reaction rate. Thirdly, in contrast to organic cations (e.g. Methylene Blue) [66], the strong electrostatic interactions between the LBL assembly blocks can result in non-uniform and defective films.

The changes in film morphology have been confirmed by SEM studies of the LBL films with different outer layers deposited onto PDDA-modified ITO glass slides (Fig. S4). Films terminated with an outer HPA layer showed the formation of uniform flake-like agglomerates with a size diameter ranging from 60 to 160 nm associated in larger islands with a mean extension of 200 nm. In a different way, films with AgNP as the outer layer displayed the presence of second aggregates domain of AgNP aggregates with an average diameter of 20 nm.

3.3. NRR and nitrite reduction on LBL films

Requiring a large overpotential at bare electrode surfaces [71], the electrochemical reduction of nitrite as one of the most reactive substances in the nitrogen cycle is effectively catalysed by the reduced W-O framework of HPA as electronic storage [31,34,44,45,47,65] to nitric oxide [55] and to further reduced products such as ammonia [48] with alleviation via the addition of transitional metal ions into the W-O cage. Nitrate is hardly reduced to nitrite in mild acidic media. Rare examples of HPA multi-substituted with transitional metal ions revealed NRR activity [49–56,58]. Here the abilities of the developed monosubstituted HPA-based films to catalyse the reduction of nitrite and NRR have been studied. Due to the inherent instability of HNO_2 (pK_a 3.3), via a disproportion reaction [72], the electrocatalytic reduction of nitrite has been studied at pH 4.5. Fig. 4 illustrates the series of cyclic voltammograms obtained for electrodes modified with Fe^{3+}- and Ni^{2+}-substituted HPAs immobilized onto the electrode surface via LBL assembly with AgNPs after successive additions of nitrite and nitrate. It can be seen that for both film-modified electrodes the reduction peak currents of both the I and II W-O redox processes increase with the additions of nitrite or nitrate, while the corresponding peak currents of oxidation decrease. Additions of nitrite or nitrate led to the appearance of comparable electrocatalytic currents on both Fe^{3+}- and Ni^{2+}-substituted HPA-based films illustrating the achievement of NRR at the same potential as nitrite electrocatalytic reduction. The voltammetric response of $Fe^{3+/2+}$ observed at around -0.05 V illustrates the presence of substituent ions inside the HPA.

However, the LBL films based upon the Cu^{2+}-substituted HPA (Fig. S5A) revealed a minor electrocatalytic effect on NRR in comparison with the Fe^{3+}- and Ni^{2+}-substituted HPA-based films.

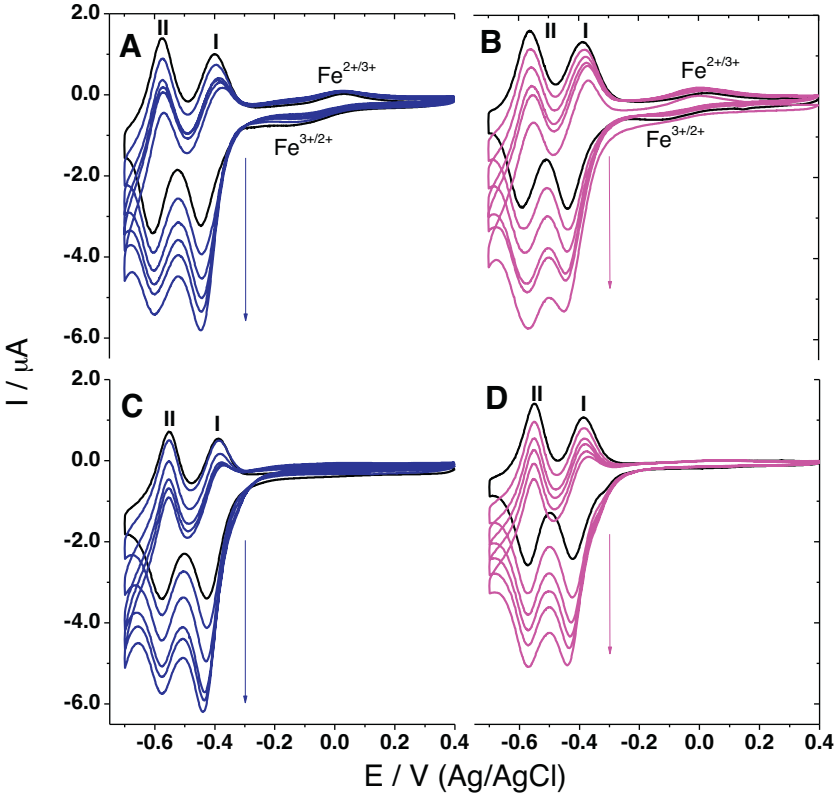

Fig. 4. Nitrite and nitrate electrocatalysis onto HPA-AgNP LBL films. Cyclic voltammograms of electrodes modified with LBL films of 16 assembly steps (AgNP as a terminal layer) with Fe^{3+}- (**A** and **B**) and Ni^{2+}-substituted (**C** and **D**) HPA recorded before (black curves) or after additions of nitrite (blue curves) or nitrate (magenta curves); 0.2 mM, 0.4 mM, 0.6 mM, 0.8 mM and 1.0 mM; pH 4.5, scan rate 10 mV/s.

W-O I redox process remained uninvolved, which was characterized with absence of changes of both reduction and oxidation peak currents for the W-O I redox process. This illustrates the significant influence of the substituent ion on the HPA's capabilities for catalysis of NRR. The electrocatalytic currents upon NRR were smaller than observed at LBL films based on crown-type HPA multi-substituted with transition metal ions [58], which illustrates the favourable effect of substituent accumulation. The crucial role of the AgNP as a cationic moiety in the LBL assembly of the active electrocatalytic film is illustrated the minor NRR activity observed with LBL film constructed with PEI and Fe^{3+}-substituted HPA (Fig. S5B). Similarly, the absence of NRR was observed at LBL films assembled with pentaerythritol-based Ru(II)-metallodendrimer and multi-substituted HPA [73,74]. Instead of the hopping conductivity observed in HPA-based LBL films assembled with cathionic insulators and characterized with the decay of electronic communication rate with the increase of number of layers [66,73,74], the AgNP-based LBL films showed the retention of communication rate with the assembly [58] probably due to the maintenance of metallic conductivity within the electrocatalytic film, which might be the main reason of NRR electrocatalysis.

The effect of the outer layer on the electrocatalytic capabilities has been observed (e.g. the comparison of Fig. 4B and Fig. S5C) and is consistent with EIS measurements. The presence of AgNP as an outer layer increases the inherent and electrocatalytic currents of the W-O I and II redox processes. The varying electrocatalytic performances of the developed LBL films towards NRR have been compared through the construction of a calibration plot (Fig. 5). Two regions of concentration dependences are distinguishable for all films. Sharp linearity region is followed by the slow increase, which probably shows the complexity of electrocatalytic process passing through the variety of intermediates. The LBL film assembled with AgNPs as the outer layer revealed the highest currents of electrocatalytic NRR. The use of AgNP in the LBL assembly led to more than 4 times increase of sensitivity for nitrate reduction ($60\,mA\,M^{-1}\,cm^{-2}$) in comparison with cationic PEI ($14.3\,mA\,M^{-1}\,cm^{-2}$) assessed in the linear range of the calibration. The films assembled with HPA as the outer layers showed up to 40% decrease of sensitivity. The correlation of sensitivity of NRR electrocatalytic currents obtained at W-O II redox process with the surface coverage assessed from the W-O I peak currents was observed, which probably illustrates the involvement of whole material in NRR electrocatalysis by redox processes at deep cathodic overpotentials.

The electrocatalytic performance of developed LBL films towards nitrite reduction has been elucidated also. Interestingly, the sufficient control of nitrite electrocatalysis by the assembly's terminal layer has been observed for the Ni^{2+}-substituted HPAs (Fig. S6A and S6B). The decrease of the overpotential and 50% higher catalytic currents for nitrite electrocatalytic reduction was achieved if the terminal layer of the LBL assembly was AgNPs due to the involvement of W-O I redox process. However, the LBL films based upon the Cu^{2+}-substituted HPAs (Fig. S6C and S6D) revealed a less prominent effect when the outer layer was either the anionic HPA or the cationic AgNPs. The Fe^{3+}-substituted HPA (Fig. S6E and S6F), as well as lacunary HPA (data not shown) showed no such effect.

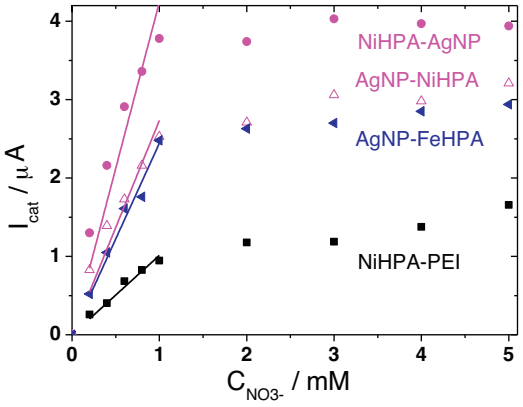

Fig. 5. Calibration plots of NRR electrocatalysis at electrodes modified by LBL films based on Fe^{3+}- or Ni^{2+}-substituted HPA with different terminal layers and cationic moieties (16 assembly steps).

Analytical characteristics of developed LBL films for nitrite reduction by W-O I and II processes have been assessed and compared with reported data (Table S1). Electrocatalysis control at the W-O I redox process of Ni^{2+}-based LBL films by terminal layer is illustrated by the 6 times increase in the sensitivity, which reached $40\,mA\,M^{-1}\,cm^{-2}$ observed. The W-O II redox process was insensitive towards the terminal layer. The LBL assembly composed of AgNPs as the cationic moiety led to sufficient increase in the sensitivity in comparison with other types of cations (PEI and pentaerythritol-based ruthenium-metallodendrimer). It is seen that in the most of the cases the elaborated LBL assembly has better performance characteristics for nitrite detection in comparison with other reported systems.

The developed systems showed the reproducibilities up to 85% and the retentions of electrocatalytic activity up to 60% to nitrate and 70% to nitrite (over a week of discontinuous measurements).

4. Conclusions

A series of Dawson-type HPA mono-substituted with transitional metal ions showed electrocatalysis to NRR and nitrite reduction being immobilized into water-processable films developed via LBL assembly with polymer-stabilized AgNP. The LBL assembly as well as the changes of HPA properties with immobilization has been characterized by electrochemical methods. On the contrast to Cu^{2+}-substituted HPA, both Fe^{3+} and Ni^{2+}-monosubstituted HPA showed the appearance of electrocatalysis to the both nitrate and nitrite reduction reactions of similar efficiencies illustrating the influence of the substituent ion of the electrocatalytic capabilities. The role of terminal layer and the cationic moiety of LBL assembly on film conductivity, morphology and electrocatalytic capabilities have been elucidated.

Acknowledgement

Authors would like to acknowledge PRDSP 2006 Program (Institute of Technology Tallaght, Dublin, Ireland) and council of Directors TSR Program Strand 3, PadovaUniversityex-60% 2012-2013-2014 and CeNano grant (Linkoping University).

References

[1] P.M. Vitousek, J.D. Aber, R.W. Howarth, G.E. Likens, P.A. Matson, D.W. Schindler, W.H. Schlesinger, D. Tilman, Human alteration of the global nitrogen cycle: Sources and consequences, Ecological Applications 7 (1997) 737–750.
[2] N. Gruber, J.N. Galloway, An Earth-system perspective of the global nitrogen cycle, Nature 451 (2008) 293–296.
[3] J.N. Galloway, A.R. Townsend, J.W. Erisman, M. Bekunda, Z.C. Cai, J.R. Freney, L. A. Martinelli, S.P. Seitzinger, M.A. Sutton, Transformation of the nitrogen cycle: Recent trends, questions, and potential solutions, Science 320 (2008) 889–892.
[4] M. Duca, M.T.M. Koper, Powering denitrification: the perspectives of electrocatalytic nitrate reduction, Energy & Environmental Science 5 (2012) 9726–9742.
[5] D.E. Canfield, A.N. Glazer, P.G. Falkowski, The Evolution and Future of Earth's Nitrogen Cycle, Science 330 (2010) 192–196.
[6] S. Hulth, R.C. Aller, D.E. Canfield, T. Dalsgaard, P. Engstrom, F. Gilbert, K. Sundback, B. Thamdrup, Nitrogen removal in marine environments: recent findings and future research challenges, Marine Chemistry 94 (2005) 125–145.

[7] N.S. Bryan, Nitrite in nitric oxide biology: Cause or consequence? A systems-based review, Free Radical Biology & Medicine 41 (2006) 691–701.
[8] C.J. Hunter, A. Dejam, A.B. Blood, H. Shields, D. Kim-Shapiro, R.F. Machado, S. Tarekegn, N. Mulla, A.O. Hopper, A.N. Schechter, G.G. Power, M.T. Gladwin, Inhaled nebulized nitrite is a hypoxia-sensitive NO-dependent selective pulmonary vasodilator, Nat. Med. 10 (2004) 1122–1127.
[9] A.V. Kozlov, B. Sobhian, C. Duvigneau, M. Gemeiner, H. Nohl, H. Redl, S. Bahrami, Organ specific formation of nitrosyl complexes under intestinal ischemia/reperfusion in rats involves nos-independent mechanism(s), Shock 15 (2001) 366–371.
[10] E.T. Reichert, S.W. Mitchell, On the Physiological Action of Potassium Nitrite, The American Journal of Medical Sciences 80 (1880) 158–180.
[11] W.H. Organization, Nitrate and Nitrite in Drinking Water, WHO Guidlines for Drinking-water Quality, World Health Organization, Geneva, 2011.
[12] W.H. Organization, Health Hazards from Nitrates in Drinking-Water, in: W.H. Organization (Ed.) Copenhagen, 1985.
[13] D.B. Kim-Shapiro, M.T. Gladwin, R.P. Patel, N. Hogg, The reaction between nitrite and hemoglobin: the role of nitrite in hemoglobin-mediated hypoxic vasodilation, Journal of Inorganic Biochemistry 99 (2005) 237–246.
[14] L. Bontoux, N., Bournis, D. Papameletiou, Options a court et a long terme pour Ie respect des normes europeenes sour les nitrates dans l'eau potable, in: E. Commission (Ed.) The IPTS Report, 1996, pp. 7.
[15] U. Prüsse, M. Hähnlein, J. Daum, K.-D. Vorlop, Improving the catalytic nitrate reduction, Catalysis Today 55 (2000) 79–90.
[16] T.C.o.t.E. Union, Council directive on the quality of water intended for human consumption, Official Journal of the European Communities, 98/83/EC (1998).
[17] A. Kapoor, T. Viraraghavan, Nitrate removal from drinking water - Review, Journal of Environmental Engineering-Asce 123 (1997) 371–380.
[18] U. Prusse, M. Hahnlein, J. Daum, K.D. Vorlop, Improving the catalytic nitrate reduction, Catalysis Today 55 (2000) 79–90.
[19] S. Horold, K.D. Vorlop, T. Tacke, M. Sell, Development of catalysts for a selective nitrate and nitrite removal from drinking water, Catalysis Today 17 (1993) 21–30.
[20] V. Rosca, M. Duca, M.T. de Groot, M.T.M. Koper, Nitrogen Cycle Electrocatalysis, Chemical Reviews 109 (2009) 2209–2244.
[21] K. Kamiya, K. Hashimoto, S. Nakanishi, Graphene Defects as Active Catalytic Sites that are Superior to Platinum Catalysts in Electrochemical Nitrate Reduction, ChemElectroChem 1 (2014) .
[22] O. Brylev, M. Sarrazin, L. Roue, D. Belanger, Nitrate and nitrite electrocatalytic reduction on Rh-modified pyrolytic graphite electrodes, Electrochimica Acta 52 (2007) 6237–6247.
[23] D. Reyter, D. Belanger, L. Roue, Study of the electroreduction of nitrate on copper in alkaline solution, Electrochimica Acta 53 (2008) 5977–5984.
[24] I. Taniguchi, N. Nakashima, K. Matsushita, K. Yasukouchi, Electrocatalytic reduction of nitrate and nitrite to hydroxylamine and ammonia using metal cyclams, Journal of Electroanalytical Chemistry 224 (1987) 199–209.
[25] E. Simon, E. Sable, H. Handel, M. L'Her, Electrodes modified by conducting polymers bearing redox sites: Ni- and Co-cyclam complexes on polypyrrole, Electrochimica Acta 45 (1999) 855–863.
[26] L. Ma, B.Y. Zhang, H.L. Li, J.Q. Chambers, Kinetics of nitrate reduction by cobalt-cyclam incorporated Nafion® redox polymer, Journal of Electroanalytical Chemistry 362 (1993) 201–205.
[27] L. Ma, H.L. Li, Electrocatalysis of adsorbed Co-cyclam at Au electrodes for nitrate reduction in concentrated alkaline solutions, Electroanalysis 7 (1995) 756–758.
[28] H.L. Li, J.Q. Chambers, D.T. Hobbs, Electrocatalytic reduction of nitrate and nitrite at Nafion®-coated electrodes in concentrated sodium-hydroxide solution, Journal of Electroanalytical Chemistry 256 (1988) 447–453.
[29] S. Kuwabata, S. Uezumu, K. Tanaka, T. Tanaka, Reduction of NO3- giving NH3 using a (BUN4N) 3 Mo2Fe6S8(SPH) 9-modified glassy carbon electrode, Journal of the Chemical Society-Chemical Communications (1986) 135–136.
[30] B. Keita, D. Bouaziz, L. Nadjo, A. Deronzier, Surface functionalization with oxometallates entrapped in polymeric matrices 2. Substituted pyrrole-based ion-exchange polymers, Journal of Electroanalytical Chemistry 279 (1990) 187–203.
[31] B. Keita, L. Nadjo, Polyoxometalate-based homogeneous catalysis of electrode reactions: Recent achievements, J. Mol. Catal. A-Chem. 262 (2007) 190–215.
[32] X.L. Wang, Q. Zhang, Z. Han, E. Wang, C. Hu, Surface-renewable graphite organosilicate composite electrode bulk-modified with a bifunctional electrocatalyst containing tris(2,2′-bipyridine) ruthenium(II) and 18-molybdosulfate, Journal of Electroanalytical Chemistry 563 (2004) 221–227.
[33] G. Bidan, E.M. Genies, M. Lapkowski, One-step electrochemical immobilization of Keggin-type heteropolyanions in poly(3-methylthiophene) films at an electrode surface - electrochemical and electrocatalytic properties, Synthetic Metals 31 (1989) 327–334.
[34] B.Q. Wang, L. Cheng, S.J. Dong, Construction of a heteropolyanion-modified electrode by a two-step sol-gel method and its electro catalytic applications, Journal of Electroanalytical Chemistry 516 (2001) 17–22.
[35] B.X. Wang, S.J. Dong, Electrochemical study of isopoly and heteropoly oxometallates film modified electrodes. 5. Preparation and electrochemical behaviour of a 2/18-molybdodiphosphate anion monolayer modified electrode, Journal of Electroanalytical Chemistry 328 (1992) 245–257.
[36] Y. Jin, L. Xu, L. Zhu, W. An, G. Gao, Nanocomposite multilayer films containing Dawson-type polyoxometalate and cationic phthalocyanine: Fabrication, characterization and bifunctional electrocatalytic properties, Thin Solid Films 515 (2007) 5490–5497.
[37] J. Tien, A. Terfort, G.M. Whitesides, Microfabrication through Electrostatic Self-Assembly, Langmuir 13 (1997) 5349–5355.
[38] M. Zynek, M. Serantoni, S. Beloshapkin, E. Dempsey, T. McCormac, Electrochemical and surface properties of multilayer films based on a Ru2+ metallodendrimer and the mixed addenda Dawson heteropolyanion, Electroanalysis 19 (2007) 681–689.
[39] N. Aihara, K. Torigoe, K. Esumi, Preparation and characterization of gold and silver nanoparticles in layered Laponite suspensions, Langmuir 14 (1998) 4945–4949.
[40] R.M. Bright, M.D. Musick, M.J. Natan, Preparation and characterization of Ag colloid monolayers, Langmuir 14 (1998) 5695–5701.
[41] D.G. Duff, A. Baiker, P.P. Edwards, A new hydrosol of gold clusters. 1. Formation and particle-size variation, Langmuir 9 (1993) 2301–2309.
[42] Y. Shiraishi, N. Toshima, Colloidal silver catalysts for oxidation of ethylene, J. Mol. Catal. A-Chem. 141 (1999) 187–192.
[43] W. Wang, S. Efrima, O. Regev, Directing oleate stabilized nanosized silver colloids into organic phases, Langmuir 14 (1998) 602–610.
[44] S. Dong, X. Xi, M. Tian, Study of the electrocatalytic reduction of nitrite with silicotungstic heteropolyanion, Journal of Electroanalytical Chemistry 385 (1995) 227–233.
[45] B. Keita, A. Belhouari, L. Nadjo, R. Contant, Electrocatalysis by polyoxometalate polymer systems - reduction of nitrite and nitric-oxide, Journal of Electroanalytical Chemistry 381 (1995) 243–250.
[46] T. McCormac, B. Fabre, G. Bidan, Role of pH and the transition metal for the electrocatalytic reduction of nitrite with transition metal substituted Dawson type heteropolyanions .2, Journal of Electroanalytical Chemistry 427 (1997) 155–159.
[47] L. Ruhlmann, G. Genet, Wells-Dawson-derived tetrameric complexes {K28H8 P2W15Ti3O60.5 (4)} electrochemical behaviour and electrocatalytic reduction of nitrite and of nitric oxide, Journal of Electroanalytical Chemistry 568 (2004) 315–321.
[48] J.E. Toth, F.C. Anson, Electrocatalytic Reduction of Nitrite and Nitric Oxide to Ammonia with Iron-Substituted Polyoxotungstates, Journal of the American Chemical Society 111 (1989) 2444–2451.
[49] L.H. Bi, U. Kortz, S. Nellutla, A.C. Stowe, J. Van Tol, N.S. Dalal, B. Keita, L. Nadjo, Structure, Electrochemistry, and Magnetism of the Iron(III)-Substituted Keggin Dimer, [Fe6(OH) 3(A-r-GeW9O34(OH) 3) 2]11-, Inorganic Chemistry 44 (2005) 896–903.
[50] D. Jabbour, B. Keita, L. Nadjo, U. Kortz, S.S. Mal, The wheel-shaped Cu20-tungstophosphate Cu20Cl(H)(24)(H2O)(12)(P8W48O184) (25-), redox and electrocatalytic properties, Electrochemistry Communications 7 (2005) 841–847.
[51] B. Keita, E. Abdeljalil, L. Nadjo, R. Contant, R. Belgiche, First examples of e•cient participation of selected metal-ion-substituted heteropolyanions in electrocatalytic nitrate reduction, Electrochemistry Communications 3 (2001) 56–62.
[52] B. Keita, I.M. Mbomekalle, L. Nadjo, Redox behaviours and electrocatalytic properties of copper within Dawson structure-derived sandwich heteropolyanions [Cu4(H2O) 2(X2W15O56)2] 16 (X = P or As), Electrochemistry Communications 5 (2003) 830–837.
[53] B. Keita, I.M. Mbomekalle, L. Nadjo, R. Contant, [H4AsW18O62]7-, A novel Dawson heteropolyanion and two of its sandwich-type derivatives [Zn4(H2O) 2(H4AsW15O56) 2]18-, [Cu4(H2O) 2(H4AsW15O56) 2]18-: cyclic voltammetry and electrocatalytic properties towards nitrite and nitrate, Electrochemistry Communications 3 (2001) 267–273.
[54] S.S. Mal, B.S. Bassil, M. Ibrahim, S. Nellutla, J. van Tol, N.S. Dalal, J.A. Fernandez, X. Lopez, J.M. Poblet, R.N. Biboum, B. Kelta, U. Kortz, Wheel-Shaped Cu-20-Tungstophosphate Cu20X(OH)(24)(H2O)(12)(P8W48O184) (25-) Ion (X = Cl, Br, I) and the Role of the Halide Guest, Inorganic Chemistry 48 (2009) 11636–11645.
[55] J. Zhang, J.K. Goh, W.T. Tan, A.M. Bond, Mechanistic analysis of the electrocatalytic properties of dissolved alpha and beta isomers of [SiW12O40] (4-) and solid [Ru(bipy)(3)](2)[alpha-SiW12O40] on the reduction of nitrite in acidic aqueous media, Inorganic Chemistry 45 (2006) 3732–3740.
[56] Y.F. Z.M. Zhang, C. Qi, Y.G. Oin, E. Li, X.L. Wang, Z.M. Wang, L. Xu Su, Two multi-copper-containing heteropolyoxotungstates constructed from the lacunary keggin polyoxoanion and the high-nuclear spin cluster, Inorganic Chemistry 46 (2007) 8162–8169.
[57] M. Ibrahim, Y. Xiang, B.S. Bassil, Y. Lan, A.K. Powell, P. de Oliveira, B. Keita, U. Kortz, Inorganic Chemistry 52 (2013) 8399–8408.
[58] S. Imar, C. Maccato, C. Dickinson, F. Laffir, M. Vagin, T. McCormac, Enhancement of Nitrite and Nitrate Electrocatalytic Reduction through the Employment of Self-Assembled Layers of Nickel and Copper-Substituted Crown-Type Heteropolyanions, Langmuir 31 (2015) 2584–2592.
[59] A.P. Ginsberg, R. Contant, W.G. Klemperer, O. Yaghi, Potassium Octadecatungstodiphosphates(V) and Related Lacunary Compounds, Inorganic Synthesis 27 (1990) 104.
[60] D.K. Lyon, W.K. Miller, T. Novet, P.J. Domaille, E. Evitt, D.C. Johnson, R.G. Finke, Highly oxidation resistant inorganic-porphyrin analog polyoxometalate oxidation catalyst. I. the synthesis and characterization of aqueouus-soluble potassium salts of alpha-2-P2W17O61(MN+.OH2)(N-10) and organic-solvent soluble tetra-normal-butylammonium salts of alpha-2-P2W17O61(MN + .BR) (N-11) (M = MN3+, FE3+, CO2+, NI2+, CU2+), Journal of the American Chemical Society 113 (1991) 7209–7221.

[61] K. Kim, H.B. Lee, J.W. Lee, K.S. Shin, Poly(ethylenimine)-stabilized silver nanoparticles assembled into 2-dimensional arrays at water–toluene interface, Journal of Colloid and Interface Science 345 (2010) 103–108.
[62] P.E. Duru, S. Bektas, O. Genc, S. Patir, A. Denizli, Adsorption of heavy-metal ions on poly(ethylene imine)-immobilized poly(methyl methacrylate) microspheres, J. Appl. Polym. Sci. 81 (2001) 197–205.
[63] Y. Zhou, R.Z. Ma, Y. Ebina, K. Takada, T. Sasaki, Multilayer hybrid films of titania semiconductor nanosheet and silver metal fabricated via layer-by-layer self-assembly and subsequent UV irradiation, Chemistry of Materials 18 (2006) 1235–1239.
[64] S.H. B.J. Wiley, Z.Y. Im, J. Li, A. McLellan, Y.N. Xia Siekkinen, Maneuvering the surface plasmon resonance of silver nanostructures through shape-controlled synthesis, Journal of Physical Chemistry B 110 (2006) 15666–15675.
[65] T. McCormac, B. Fabre, G. Bidan, Part I. A comparative electrochemical study of transition metal substituted Dawson type heteropolyanions, Journal of Electroanalytical Chemistry 425 (1997) 49–54.
[66] N. Anwar, M. Vagin, R. Naseer, S. Imar, M. Ibrahim, S.S. Mal, U. Kortz, F. Laffir, T. McCormac, Redox Switching of Polyoxometalate-Methylene Blue based Layer-by-Layer Films, Langmuir 28 (2012) 5480–5488.
[67] W.Y. Tao, Z.F. Li, D.W. Pan, L.H. Nie, S.Z. Yao, Preparation, structure, and electrochemistry of a polypyrrole film doped with manganese(III)-substituted Dawson-type phosphopolyoxotungstate, Journal of Physical Chemistry B 109 (2005) 2666–2672.
[68] M. Ammam, B. Keita, L. Nadjo, I.M. Mbomekalle, J. Fransaer, Attempts to immobilize catalytically active substituted-heteropolytungstates in multilayer film of charged polyelectrolyte poly(allylamine hydrochloride), Journal of Electroanalytical Chemistry 645 (2010) 65–73.
[69] Y. H. Ma, Z. Gu, H. Zhang, S. Pang, L. Kang Li, Enhanced electrocatalytic activity of a polyoxometalates-based film decorated by gold nanoparticles, Electrochimica Acta 56 (2011) 7428–7432.
[70] R.J. Stanis, M.C. Kuo, A.J. Rickett, J.A. Turner, A.M. Herring, Investigation into the activity of heteropolyacids towards the oxygen reduction reaction on PEMFC cathodes, Electrochimica Acta 53 (2008) 8277–8286.
[71] M.H. Bradley, M.R. Rhodes, T.J. Meyer, Electrocatalytic reduction of nitrite to nitrous oxide and ammonia based on the N-methylated, cationic iron porphyrin complex [FeIII(H2O)(TMPyP)]5+, Inorganic Chemistry 26 (1987) 1746–1750.
[72] N. Fay, E. Dempsey, T. McCormac, Assembly, electrochemical characterisation and electrocatalytic ability of multilayer films based on Fe(bpy)(3) (2+), and the Dawson heteropolyanion, P2W18O62 (6-), Journal of Electroanalytical Chemistry 574 (2005) 359–366.
[73] R. Naseer, S.S. Mal, M. Ibrahim, U. Kortz, G. Armstrong, F. Laffir, C. Dickinson, M. Vagin, T. McCormac, Redox, surface and electrocatalytic properties of layer-by-layer films based upon Fe(III)-substituted crown polyoxometalate [P8W48O184Fe16(OH) 28(H2O) 4]20-, Electrochimica Acta 134 (2014) 450–458.
[74] R. Naseer, S.S. Mal, U. Kortz, G. Armstrong, F. Laffir, C. Dickinson, M. Vagin, T. McCormac, Electrocatalysis by crown-type polyoxometalates multi-substituted by transition metal ions; Comparative study, Electrochimica Acta 176C (2015) 1248–1255.